Journal of Zhejiang University-SCIENCE B 2025 26(12):1216-1232
www.jzus.zju.edu.cn; www.springer.com/journal/11585
E-mail: jzus_b@zju.edu.cn

Research Article
https://doi.org/10.1631/jzus.B2400509

Depleting CBR1 increases chemosensitivity by reducing stemness and quiescence traits in non-small cell lung cancer

Weiwen LI[1,2], Jialu ZHAO[2], Weihong LAN[2], Xiaofei YE[2], Kejing YING[1]✉

[1]*Department of Respiratory and Critical Medicine, Sir Run Run Shaw Hospital, Zhejiang University School of Medicine, Hangzhou 310016, China*
[2]*Department of Respiratory and Critical Medicine, The Fifth Affiliated Hospital to Wenzhou Medical University, Lishui 323000, China*

Abstract: Carbonyl reductase 1 (CBR1), a member of the short-chain dehydrogenase/reductase (SDR) superfamily, is implicated in tumor progression and treatment resistance. However, its role in non-small cell lung cancer (NSCLC) remains unclear. This study examined CBR1 expression in NSCLC tissues and cell lines, using gene interference and pharmacological inhibition to assess its impact on stemness, chemosensitivity, and quiescence, and to explore underlying mechanisms. Our findings indicate that CBR1 expression is elevated in NSCLC tissues and cell lines, and further increases in the presence of cisplatin (CDDP). Gene interference reducing CBR1 expression significantly decreased the percentage of cluster of differentiation 133 (CD133)-positive cells and the expression of octamer-binding transcription factor 4 (OCT4) and SRY (sex determining region Y)-box 2 (SOX2), while enhancing CDDP chemosensitivity. The CBR1-specific inhibitor hydroxy-PP-Me (PP-Me) markedly increased CDDP cytotoxicity and reduced stemness. Additionally, CBR1 inhibition via short hairpin RNA (shRNA) CBR1 (sh-CBR1) or PP-Me disrupted NSCLC cell quiescence, as shown by a decrease in G0 phase cells and p27 expression, alongside an increase in cyclin D1 and phospho-retinoblastoma (pRb) expression. Furthermore, SET domain-containing protein 4 (SETD4), which mediates stemness, chemosensitivity, and quiescence in NSCLC cells, was downregulated by sh-CBR1 or PP-Me treatment. The overexpression of SETD4 counteracted the enhanced chemosensitivity resulting from CBR1 inhibition. In A549 xenografts, combined PP-Me and CDDP therapy significantly inhibited tumor growth compared to either treatment alone. In conclusion, CBR1 inhibition enhances CDDP chemosensitivity by suppressing stemness and quiescence in NSCLC.

Key words: Carbonyl reductase 1 (CBR1); SET domain-containing protein 4 (SETD4); Chemosensitivity; Stemness; Quiescence; Non-small cell lung cancer (NSCLC)

1 Introduction

Lung cancer remains a prominent cause of cancer-related mortality globally, with nearly 2 million new cases diagnosed annually (Brody, 2020; Siegel et al., 2021). Non-small cell lung cancer (NSCLC), in particular, imposes a substantial burden on patients and their families (Brody, 2020; Siegel et al., 2021). Despite significant advancements in diagnosis and treatment, many patients still experience treatment failure and relapse (Brody, 2020). Chemotherapy remains one of the main treatment modalities used for NSCLC. It can be used as a primary treatment for NSCLC, especially in cases where surgery is not possible or the cancer has spread to other parts of the body. Chemotherapy can also be used in combination with other treatments such as surgery, radiation therapy, targeted therapy, and immunotherapy to achieve better outcomes (Miller and Hanna, 2021). Despite the initial effectiveness of chemotherapy, tumor recurrence can occur due to several factors, such as the presence of cancer stem cells (CSCs), genetic mutations, metabolism reprogramming, and alternative signaling pathways (Chen et al., 2023b; Zhang et al., 2023a). Effective strategies need to be developed to increase chemotherapy sensitivity, and the underlying mechanisms need to be investigated.

CSCs, also known as tumor-initiating cells, are a subpopulation of cells within a tumor that have stem cell-like properties, including self-renewal and the ability to give rise to diverse cell types within the tumor. The presence of CSCs is a major obstacle to effective

✉ Kejing YING, 3197061@zju.edu.cn
Kejing YING, https://orcid.org/0000-0002-6396-4339

Received Oct. 14, 2024; Revision accepted Jan. 6, 2025;
Crosschecked Dec. 12, 2025; Published online Dec. 17, 2025

treatment, including chemotherapy (Heng et al., 2019). These cells often have enhanced DNA repair mechanisms, lower rates of cell division, and increased expression of drug efflux pumps, all of which can contribute to their resistance to chemotherapy agents (Heng et al., 2019). CSCs can enter a quiescent state as a survival strategy, which can have significant implications for cancer progression, treatment resistance, and the potential for tumor recurrence (Ye et al., 2019; Mukhopadhyay et al., 2023; Wang et al., 2023). The quiescent cells temporarily arrest the cell cycle in the G0 phase and cease dividing. This is accompanied by alterations in G0/G1-related proteins, including decreased cyclin D1 and phospho-retinoblastoma (pRb) but increased p27 (Jiang et al., 2020; Pennycook and Barr, 2020; Massey et al., 2021). In the context of cancer cells, the ability to enter and exit quiescence is an important aspect of their behavior. Quiescent cancer cells retain the potential to re-enter the active cell cycle, contributing to tumor recurrence and regrowth after treatment. Apart from cell cycle arrest, quiescent CSCs show resistance to apoptosis, altered metabolism, and genetic and epigenetic changes (Chen et al., 2021).

Recently, epigenetic modifications were identified as novel alterations in quiescent CSCs, contributing to their resistance to therapy and their ability to self-renew. SET domain-containing protein 4 (SETD4), a histone methyltransferase, has gained increasing attention. A subset population of SETD4-positive quiescent CSCs is responsible for chemotherapy resistance by modifying DNA methylation processes and influencing chromatin remodeling (Ye et al., 2019). Indeed, SETD4 has been established as a functional readout of quiescence in CSCs (Mukhopadhyay et al., 2023), and its inhibition has been shown to enhance chemosensitivity (Wang et al., 2023). SETD4 regulates chromatin structure, gene expression, and essential cellular processes such as cell cycle progression, gene transcription, and DNA repair (Herz et al., 2013). It plays a pivotal role in maintaining cellular homeostasis, particularly in CSCs, which are characterized by their ability to remain dormant in a quiescent state. The dysregulation of SETD4 may play a crucial role in sustaining the quiescent state of CSCs, facilitating tumor progression, and promoting resistance to therapy (Herz et al., 2013). SETD4's involvement in NSCLC has been increasingly recognized, with evidence suggesting that its dysregulation may contribute to tumorigenesis, metastasis, and therapeutic resistance (Wang et al., 2023). Recent studies indicate that SETD4 is a potential biomarker and therapeutic target, highlighting its significance in both the biology of CSCs and the clinical challenges associated with treating this aggressive cancer (Herz et al., 2013; Wang et al., 2023). Ongoing research is focused on identifying specific markers and vulnerabilities in both actively dividing and quiescent CSC populations. By targeting these vulnerabilities, new therapeutic strategies could be developed to selectively eliminate CSCs and overcome resistance mechanisms. Thus, understanding the role of SETD4 in CSC quiescence and its potential for therapeutic targeting is of paramount importance.

Even in a non-dividing state, quiescent cells need to maintain cellular integrity and perform essential cellular functions by modulating cellular metabolism. This includes reduced glycolysis, increased fatty acid oxidation, altered nucleotide metabolism, and maintenance of redox balance (Chen et al., 2021). Importantly, the short-chain dehydrogenase/reductase (SDR) superfamily is involved in the oxidation and reduction of a wide range of substrates, contributing to various metabolic pathways and tumor progression (Kavanagh et al., 2008; Bray et al., 2009). Carbonyl reductase 1 (CBR1) is an enzyme that belongs to the SDR superfamily (Oppermann, 2007). CBR1 acts on a variety of substrates and is involved in the reduction of carbonyl groups in substances, which may induce cellular stress (Oppermann, 2007). CBR1 is implicated in the metabolism of chemotherapeutic agents, removing them from the body (Lal et al., 2008; Koczurkiewicz-Adamczyk et al., 2020, 2022). Due to the ability to reduce carbonyl-containing compounds, including those generated during oxidative stress, the presence of CBR1 may provide a survival advantage to cancer cells (Koczurkiewicz-Adamczyk et al., 2022). Studies have reported that CBR1 is upregulated in various cancers compared to normal tissue, participates in signal transduction and apoptosis, and contributes to treatment resistance in cancer (Tak et al., 2011; Jang et al., 2012; Piska et al., 2019; Koczurkiewicz-Adamczyk et al., 2022). However, its roles and mechanism in maintaining the properties of CSCs and chemotherapy resistance in NSCLC remain unclear.

In this study, our main objective was to investigate the effects of CBR1 on cancerous phenotypes of CSCs in NSCLC and its influence on sensitivity to

cisplatin (CDDP). First, we verified the high expression and poor prognosis of CRB1 using The Cancer Genome Atlas (TCGA) data and clinical samples, as well as NSCLC cell lines. Gene interference and pharmacological inhibition strategy of CBR1 were used to confirm oncogenic effects including proliferation, stemness, quiescence, and CDDP resistance. Furthermore, we applied a gene overexpression strategy to maintain the expression of SETD4, a functional readout of quiescence in CSCs (Ye et al., 2019; Mukhopadhyay et al., 2023), to verify the enhanced chemosensitivity of CBR1 inhibition in quiescent cells. Finally, a xenograft tumor model was used to confirm the enhanced chemosensitivity of CBR inhibition in vivo. Overall, we aimed to demonstrate that CBR1 inhibition enhances chemosensitivity by suppressing stemness and quiescence in NSCLC. Our findings may aid in the discovery of biomarkers that predict treatment outcomes in NSCLC and the development of personalized treatments, and pave the way for targeted therapies aimed at reducing cancer stemness and quiescence in NSCLC.

2 Materials and methods

2.1 Reagents and antibodies

Cisplatin (CAS No. 15663-27-1) was purchased from Med Chem Express (Shanghai, China). SETD4 (sc-514060) antibody was obtained from Santa Cruz Biotechnology (Shanghai, China). Antibodies against Ki67 (ab16667) and CBR1 (ab156590) were obtained from Abcam (Shanghai, China). Antibodies against SRY (sex determining region Y)-box 2 (SOX2) (#3579), octamer-binding transcription factor 4 (OCT4) (#2750), glyceraldehyde 3-phosphate dehydrogenase (GAPDH) (#2118), pRb (#8516), β-actin (#3700), as well as horseradish peroxidase (HRP)-linked anti-rabbit immunoglobulin G (IgG) (#7074) secondary antibody, were purchased from Cell Signaling Technology (Shanghai, China). Cyclin D1 (60186-1-Ig) and p27 (25614-1-AP) were obtained from Proteintech (Shanghai, China). Phycoerythrin (PE) anti-human cluster of differentiation 133 (CD133) antibody (S16015F) was obtained from Biolegend (San Diego, CA, USA). A BeyoClick™ 5-ethynyl-2'-deoxyuridine (EdU) cell proliferation kit with Alexa Fluor 555 (C0075S) and an enhanced cell counting kit-8 (CCK-8) (C0041) were purchased from Beyotime Biotechnology (Shanghai, China).

2.2 Lung cancer cell lines and quiescent cell model development

A panel of lung cancer cell lines (PC9, H661, H1975, A549, and H1229) and human bronchial epithelial (HBE) cells were used. These cells were cultured in either Dulbecco's modified Eagle's medium (DMEM) or Roswell Park Memorial Institute (RPMI) 1640 medium (Gibco, Shanghai, China), supplemented with 10% (volume fraction) fetal bovine serum (FBS) and 100 μg/mL penicillin and streptomycin (Sigma, Shanghai, China). Upon reaching 80%–90% confluence, the cells were detached using 2.5% (0.025 g/mL) trypsin ethylenediaminetetraacetic acid (EDTA) (Sigma) and resuspended in fresh medium for passage. Subsequently, the cells were incubated at 37 ℃ with 5% CO_2, and the culture medium was refreshed every 2 to 3 d. To develop a quiescent cell model, the medium in which cells reached a confluence of 70%–80% was changed to 0.2% FBS medium and the cells were cultured for another 3 or 7 d.

2.3 TCGA database analysis

The messenger RNA (mRNA) profile of CBR1 was extracted from the TCGA database (https://www.cancer.gov/ccg/research/genome-sequencing/tcga). Differential expression analysis of CBR1 was conducted, considering sample types, individual cancer stages, and nodal metastasis status, using online tools and resources (https://ualcan.path.uab.edu). The overall survival (OS) and post-operative progression-free survival (PPS) of patients with low or high expression of CBR1 were compared using Kaplan-Meier survival analysis (https://kmplot.com).

2.4 Cell transfection

Short hairpin RNA (shRNA)-encoding sequences targeting SETD4 (sh-SETD4, sc-153385) and CBR1 (sh-CBR1, sc-390554) from Santa Cruz Biotechnology were used to downregulate SETD4 or CBR1 expression. An empty sequence served as the negative control (sh-nc). To increase the expression of SETD4, a pLKD-CMV-GPR-U6-puromycin vector containing SETD4 from Ribobio (Shanghai, China) was used. A corresponding empty vector was used as the control. Briefly, A549 and PC9 cells were transfected with shRNA and an equal volume of sh-nc. The second transfection was performed after allowing sufficient time

for the expression of the first plasmid. Subsequently, the vector containing SETD4 and its corresponding empty vector were added to sh-CBR1-infected A549 and PC9 cells. Positive cells were selected using puromycin (5 μg/mL) (Invitrogen, Shanghai, China). The expression of targeted proteins was verified using western blot analysis.

2.5 Cell viability assay

Cell viability was assessed using CCK-8, following the methods reported in a previous study (Chen et al., 2023a). Briefly, 3×10^3 cancer cells/well were seeded in 96-well plates. The cells were then subjected to the indicated treatments and incubated at 37 ℃ with 5% CO_2 for 48 h. Subsequently, 20 μL of CCK-8 solution was added to each well and incubated at 37 ℃ for 1 h. The absorbance of the cells was measured using a microplate reader (BioTek, Winooski, VT, USA) for analysis.

2.6 EdU staining assay

The BeyoClick™ EdU cell proliferation kit with Alexa Fluor 555 (Beyotime Biotechnology) was used following the manufacturer's instructions. First, shRNA- or sh-nc-infected cells were fixed in 4% (0.04 g/mL) paraformaldehyde. Next, 0.3% (volume fraction) Triton X-100 was added to permeabilize the cells. Subsequently, the appropriate amount of EdU solution was added for EdU staining. To visualize the nuclei, 4',6-diamidino-2-phenylindole (DAPI) staining was performed. The positive cells were then observed and analyzed using a microscope (Leica DMi8, Wetzlar, Germany).

2.7 Colony formation assay

About 500 shRNA- or sh-nc-infected cancer cells per well were seeded into 6-well plates. The cells were then incubated at 37 ℃ with 5% CO_2, and the culture medium was refreshed every three days. After two weeks, the clonal nodules were stained using a 0.2% (0.002 g/mL) crystal violet solution (Beyotime Biotechnology). The colonies were manually counted to assess their growth and formation.

2.8 Sphere formation

To obtain CSCs, shRNA- or sh-nc-infected cancer cells (2×10^4 cells/well) were seeded in ultralow attachment 24-well plates (Corning Inc., Corning, NY, USA). The cells were cultured in serum-free DMEM/F12 medium (Gibco, Carlsbad, CA, USA) supplemented with commercial hormone mix B27 (Gibco), 10 ng/mL basic fibroblast growth factor (bFGF), 20 ng/mL epidermal growth factor (EGF) (Sigma-Aldrich, St. Louis, MO, USA), and 1× B27 (Invitrogen). The cells were then incubated at 37 ℃ with 5% CO_2 for 7 d to promote sphere formation. Spheres of more than 50 cells or larger were counted, and representative images were captured using a microscope (Leica DMi8).

2.9 Flow cytometry analysis of CD133

The cells with the indicated treatment were harvested and prepared into suspension. The cells were fixed and permeabilized. Then, 2% (0.02 g/mL) bovine serum albumin (BSA) (in phosphate-buffered saline (PBS)) was added to block non-specific binding sites for 30 min. Diluted primary antibody (a volume ratio of 1:500) was added to the cell suspension which was then incubated for 1–2 h at room temperature or overnight at 4 ℃. Unbound secondary antibodies were removed. Stained cells were analyzed using a flow cytometer (BD FACSCanto, USA), adjusting voltage and compensation settings as needed. FlowJo software was used to analyze the flow cytometry data and gate populations based on fluorescence intensity.

2.10 Cell cycle distribution analysis

A cell cycle analysis kit (Beyotime Biotechnology) was used to analyze the cell cycle distribution according to the manufacturer's instructions. Briefly, the cells were harvested and resuspended in PBS. The resuspended cells were washed twice and the collected cells were fixed with 70% (volume fraction) alcohol at 4 ℃ overnight. Next, 10 μL RNase A (50×) and 25 μL propidium were added to 0.5 mL binding buffer to obtain the staining buffer. The cells were incubated with the staining buffer for 30 min at 37 ℃. Then, the cell cycles were analyzed using flow cytometry (BD FACSCanto).

2.11 Immunocytochemistry

Immunocytochemistry was conducted following methods reported in a previous study (Zhang et al., 2023b). sh-CBR1- or sh-nc-infected cancer cells were seeded on slides in 6-well plates. The cells were fixed in 4% paraformaldehyde for 10 min at room temperature. To permeabilize the cells, 0.25% Triton

X-100 was added and incubated for 10 min. To block unspecific binding of antibodies, 1% BSA was added and allowed to incubate for 30 min. Subsequently, the cells were exposed to the primary antibody solution (SETD4, a volume ratio of 1:500) and incubated overnight at 4 ℃. The next day, the cells were incubated with the secondary antibody in 1% BSA for 1 h at room temperature in the dark. For nuclear staining, 1 μg/mL of DAPI was added. The positive cells were then visualized and observed using a microscope (Leica DMi8).

2.12 Western blot analysis

Cells with the indicated treatment were lysed using radioimmunoprecipitation assay (RIPA) lysis buffer (Beyotime Biotechnology), and total protein was collected. The tissue samples were homogenized in ice-cold lysis buffer. The tissue was disrupted using a tissue homogenizer until a fine suspension was achieved. After homogenization, the samples were incubated on ice for 30 min with intermittent mixing. The lysates were then centrifuged at 12 000*g* for 15 min at 4 ℃ to remove cellular debris. The supernatant containing the soluble protein fraction was collected, and the protein concentration was measured using a Bradford protein concentration assay kit (Beyotime Biotechnology). Protein extracts were stored at −80 ℃ for further analysis. For protein separation, equal amounts of protein were loaded onto a sodium dodecyl sulfate-polyacrylamide gel electrophoresis (SDS-PAGE) for separation. Polyvinylidene fluoride (PVDF) membranes (Millipore, Bedford, MA, USA) were used to transfer the separated proteins. Subsequently, the membranes were blocked with 5% (volume fraction) nonfat milk and incubated with primary antibodies overnight at 4 ℃. The corresponding secondary antibodies were then added to the membranes, and the proteins were visualized using enhanced chemiluminescence (Bio-Rad Laboratories Co., Ltd., Shanghai, China).

2.13 Xenograft model

All animal experiments were conducted with the approval of the experimental animal ethical committee of The Fifth Affiliated Hospital to Wenzhou Medical University. BALB/c nude mice (Shanghai SLAC Laboratory Animal Co., Ltd., Shanghai, China) were anesthetized using isoflurane (Shanghai Abbott Pharmaceutical Co., Ltd., Shanghai, China). Subsequently, a total of 5×10^6 A549 cells were injected subcutaneously into the left upper back of each mouse. The mice were then divided into four groups: a control group, PP-Me group, CDDP group, and a PP-Me plus CDDP group. The doses of PP-Me and CDDP were 30 mg/kg and 1 mg/kg, respectively. Tumor size was manually monitored every three days using calipers. The tumor volume (V) was calculated using the formula $V=L\times W^2/2$; L and W represent the length and width of tumor, respectively. At 21 d, the mice were sacrificed, and the tumor masses were collected. Western blot analysis was performed to detect the expression of SOX2, OCT4 and SETD4 in each group.

2.14 Statistical analysis

Statistical analysis was performed using GraphPad 8.0 software (San Diego). The data are presented as mean±standard deviation (SD). Differences between groups were evaluated using analysis of variance (ANOVA) followed by Tukey's post hoc analysis. P values less than 0.05 were considered statistically significant.

3 Results

3.1 Expression of CBR1 and pro-proliferative effect in NSCLC

The mRNA expression profile from the TCGA database revealed that the expression of *CBR1* is upregulated in NSCLC tissues from patients at both early and advanced stages (Figs. S1a and S1b). Furthermore, patients with nodal metastasis status showed higher expression levels of *CBR1* than healthy individuals (Fig. S1c). To validate the expression of CBR1 in NSCLC, western blot analysis was performed on non-tumor and tumor tissues obtained from five patients. Consistent with a previous study (Schlager and Powis, 1990), the protein expression of CBR1 was higher in NSCLC tumor tissues than in adjacent non-tumor tissues (Figs. 1a and 1b). Additionally, our findings indicated that NSCLC cell lines exhibit higher levels of CBR1 expression than HBE cells (Figs. 1c and 1d). These results strongly suggest that CBR1 is indeed overexpressed in both NSCLC tissues and cell lines. To obtain the prognostic value of CBR1 in NSCLC, survival data from the TCGA database were analyzed. The results suggested that patients with high expression of CBR1 had shorter OS and PPS (Figs. S1d and

S1e). Among patients receiving chemotherapy with high CBR1 expression, the OS and PPS were further shortened, highlighting its prognostic value for both survival and treatment response (Figs. S1f and S1g). Considering that the highest expression of CBR1 was observed in A549 and PC9 cells, these cell lines were used for further investigation (Figs. 1c and 1d). To elucidate the potential malignant functions of CBR1, a gene interference strategy was used to knock down CBR1 expression in A549 and PC9 cells (Fig. 1e). Subsequently, in sh-CBR1-infected cells, we found significant decreases in cell viability (Fig. 1f), the number of colonies (Figs. 1g and 1h), and the proportion of EdU-positive cells (Figs. 1i and S1h), demonstrating its inhibitory effects on growth.

3.2 Stemness-promoting effect of CBR1

Next, we treated lung cancer cells with a stemness inducer to investigate the effect of CBR1 on tumor stemness. As shown in Figs. 2a and 2b, the CSCs of NSCLC exhibited a higher percentage of CD133-positive cells. The expression of the two other CSC markers, SOX2 and OCT4, was increased, as shown by western blots (Figs. 2c and 2d). The expression of CBR1 was found to be higher in CSCs than in non-CSCs (Figs. 2c and 2d). Furthermore, CBR1 inhibition using

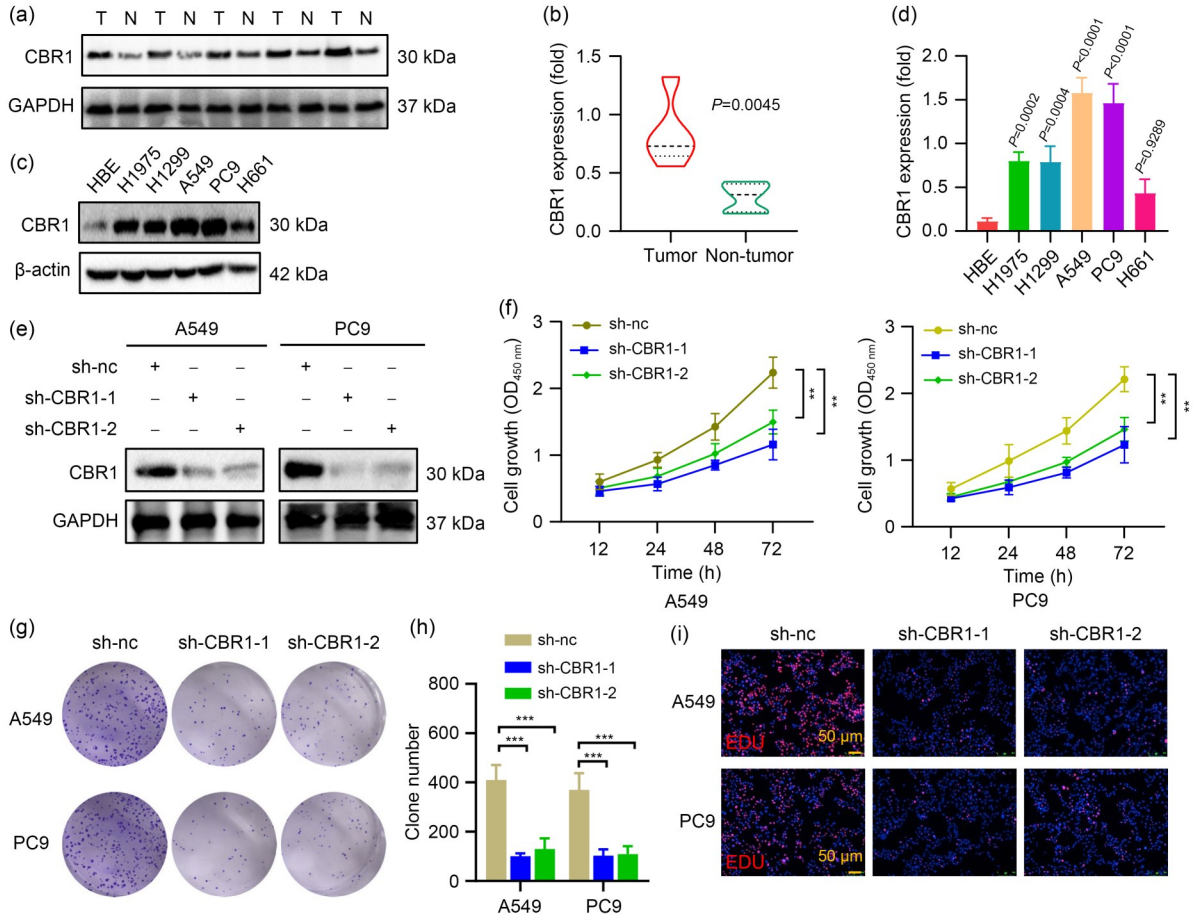

Fig. 1 Expression and oncogenic effects of CBR1 in NSCLC. (a) The expression of CBR1 in non-tumor and tumor samples from five patients was tested using western blotting. (b) Statistical analysis of CBR1 in non-tumor and tumor tissues (n=5). (c) The expression of CBR1 in NSCLC cell lines and human bronchial epithelial (HBE) cells was tested using western blotting. (d) Statistical analysis of CBR1 in cell lines (P value, vs. HBE). (e) Gene interference strategy applied to knock down the expression of CBR1. (f) Cell viability tested using CCK-8 assay. (g) Visualization of clones. (h) Statistical analysis of the number of clones. (i) Visualization of EdU-positive cells. (d, f, h) The data were expressed as mean±SD, n=3. One-way ANOVA with Dunnett's multiple comparisons test was used. ** P<0.01, *** P<0.001. T: tumor; N: non-tumor; CBR1: carbonyl reductase 1; NSCLC: non-small cell lung cancer; sh-nc: short hairpin RNA (shRNA) negative control; sh-CBR1: shRNA CRB1; GAPDH: glyceraldehyde-3-phosphate dehydrogenase; CCK-8: cell counting kit-8; EdU: 5-ethynyl-2'-deoxyuridine; ANOVA: analysis of variance; SD: standard deviation.

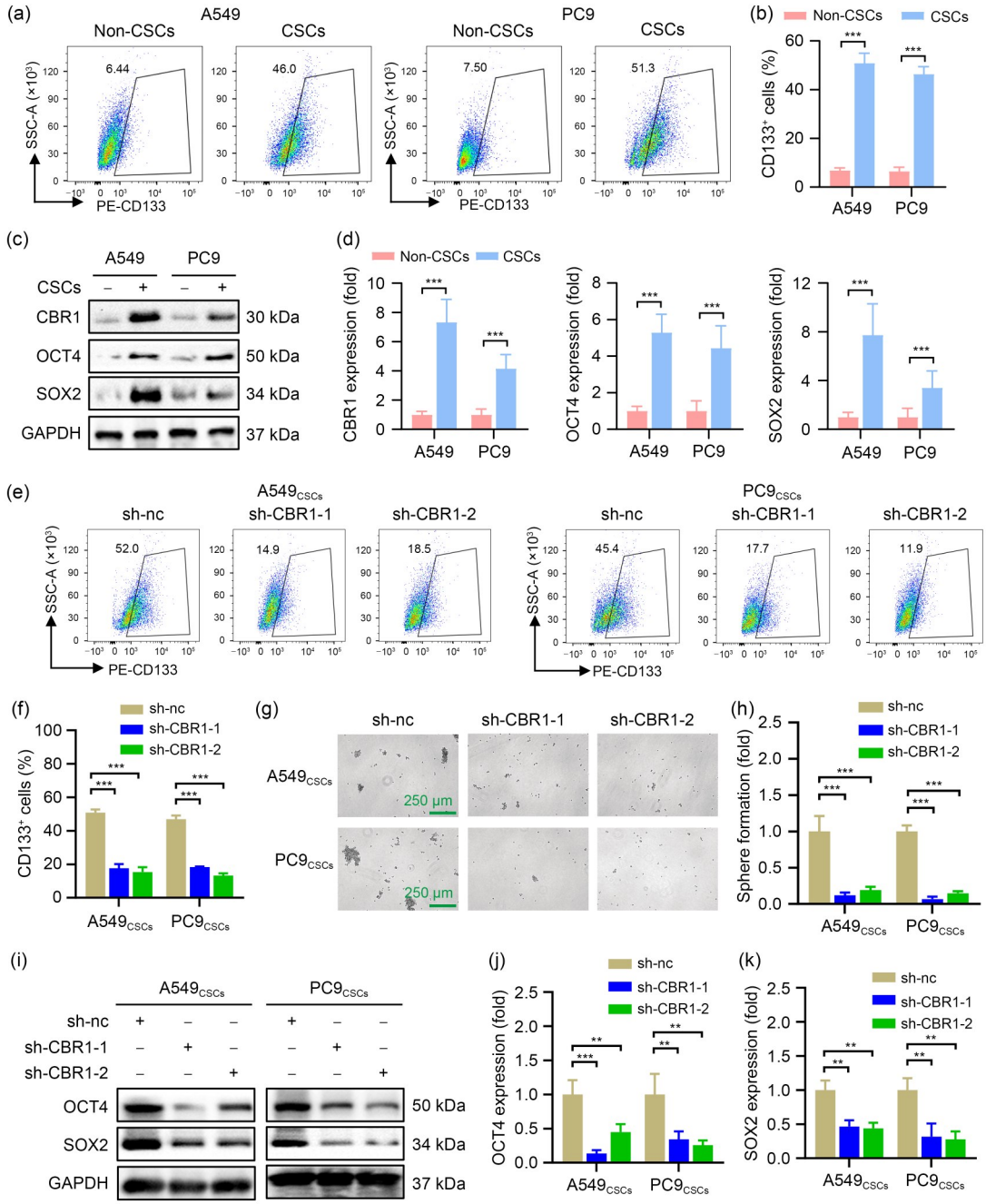

Fig. 2 Ability of CBR1 to maintain the stemness property of NSCLC cells. (a) FCM analysis of CD133-positive cells in non-CSCs and CSCs. (b) The percentage of CD133-positive non-CSCs and CSCs. (c) Western blot analysis of CBR1 and the stem cell markers OCT4 and SOX2. (d) Statistical analysis of the expression of CBR1, OCT4, and SOX2. (e) FCM analysis of CD133-positive sh-CBR1-1- and sh-CBR1-2-infected CSCs. (f) The percentage of CD133-positive sh-CBR1-1- and sh-CBR1-2-infected CSCs. (g) Representative images of sphere formation in sh-CBR1-1- and sh-CBR1-2-infected CSCs. (h) Relative sphere formation ability of sh-CBR1-1- and sh-CBR1-2-infected CSCs. (i) Western blot analysis of OCT4 and SOX2. (j, k) Statistical analysis of the expression of OCT4 (j) and SOX2 (k). The data were expressed as mean±SD, *n*=3. One-way ANOVA with Dunnett's multiple comparisons test was used. ** *P*<0.01, *** *P*<0.001. CSCs: cancer stem cells; CBR1: carbonyl reductase 1; NSCLC: non-small cell lung cancer; FCM: flow cytometry; CD133: cluster of differentiation 133; OCT4: octamer-binding transcription factor 4; SOX2: SRY (sex determining region Y)-box 2; sh-nc: short hairpin RNA (shRNA) negative control; sh-CBR1: shRNA CRB1; ANOVA: analysis of variance; SD: standard deviation; GAPDH: glyceraldehyde-3-phosphate dehydrogenase; $A549_{CSCs}$: cancer stem cells derived from A549; $PC9_{CSCs}$: cancer stem cells derived from PC9; PE-CD133: phycoerythrin-conjugated antibody of CD133; SSC-A: side scatter-area.

a gene interference strategy led to a sharp decrease in the number of CD133-positive A549 and PC9 CSCs (Figs. 2e and 2f). The ability of A549 and PC9 cells to form spheres declined in sh-CBR1-infected cells (Figs. 2g and 2h). The western blot results confirmed that the expression of OCT4 and SOX2 was decreased in sh-CBR1-infected A549 and PC9 cells compared to the corresponding negative control plasmid (Figs. 2i–2k). These findings suggest that CBR1 plays an essential role in maintaining the stem cell-like property of NSCLC cells.

3.3 Enhanced chemosensitivity induced by CBR1 inhibition in NSCLC cells

Subsequently, we investigated whether CBR1 inhibition enhanced the chemosensitivity of NSCLC cells to CDDP. The indicated concentrations of CDDP were added to A549 and PC9 cells infected with sh-CBR1. The half maximal inhibitory concentration (IC_{50}) of sh-CBR1-infected cells to CDDP declined from 10.69 to 3.61 μmol/L in A549 cells and from 9.93 to 3.12 μmol/L in PC9 cells (Fig. 3a). Similarly, PP-Me treatment decreased the IC_{50} of CDDP from 10.14 to 3.96 μmol/L in A549 cells and from 9.74 to 4.03 μmol/L in PC9 cells (Fig. 3b). Indeed, the expression of CBR1 was upregulated in NSCLC cells exposed to 2.0 μmol/L CDDP without exhibiting cytotoxicity (Figs. 3c and 3d). For validation, the inhibitory effects of combined therapy of PP-Me and 5.0 μmol/L CDDP, a dosage with less than 20% cytotoxicity, were tested using CCK-8 and EdU assays. Compared to CDDP treatment alone, the combined therapy resulted in a sharp decrease in cell viability (Fig. 3e) and the percentage of EdU-positive cells (Figs. 3f and 3g). Furthermore, the percentage of CD133-positive cells was lower in cells treated with PP-Me and CDDP than in A549 and PC9 cells treated with CDDP alone (Figs. 3h and S2a). Additionally, the expression of OCT4 and SOX2 declined significantly in A549 and PC9 cells treated with PP-Me and CDDP (Figs. 3i, S2b, and S2c). These findings strongly suggest that CBR1 inhibition enhances the chemosensitivity of NSCLC cells to CDDP.

3.4 CBR1-induced quiescence in NSCLC cells

CSCs may enter a state of quiescence, exhibiting reduced sensitivity to chemotherapeutic agents (Ye et al., 2019; Mukhopadhyay et al., 2023; Wang et al., 2023). Based on its capacity to maintain stemness and increase chemotherapy resistance, we sought to determine whether CBR1 promotes quiescence. For this purpose, we initially developed a quiescent cell model by incubating NSCLC cells in medium containing 0.2% FBS instead of the usual 10% for 7 d, as reported previously (Jiang et al., 2020). As expected, the quiescent cells exhibited G0 phase arrest, with an approximately 15% increase in G0 cells (Figs. 4a and 4b). The western blot results confirmed that the expression of cell cycle progression-related proteins, including pRb and cyclin D1, was reduced in quiescent cells incubated in 0.2% FBS medium for 3 or 7 d. However, the expression of p27, a marker of quiescent cells, was much higher than that of normal cells (Figs. 4c and S3a–S3c). We also found that the expression of SETD4, a functional readout of quiescence related to CSCs, was increased in quiescent cells (Figs. 4c and S3d). These results show that the model can be used as a quiescent cell model. Furthermore, our results indicated that the expression of CBR1 was upregulated in quiescent cells (Figs. 4c and S3e). We also observed a significant decrease in G0 cells in PP-Me-treated or sh-CBR1-infected quiescent cells (Figs. 4d and 4e). The western blot results confirmed that the expression of pRb and cyclin D1 increased in PP-Me-treated or sh-CBR1-infected quiescent cells, while the expression of p27 and SETD4 decreased (Figs. 4f and S3f–S3i). To investigate the mechanism, we focused on the roles of SETD4 in CBR1-mediated quiescence, given the previously reported capacity of SETD4 to regulate quiescence in CSCs (Mukhopadhyay et al., 2023; Wang et al., 2023). Indeed, *SETD4* mRNA expression was positively associated with *CBR1* mRNA expression in NSCLC samples from the TCGA database (Fig. 4g). Our quantitative polymerase chain reaction (qPCR) and immunofluorescence staining results verified that SETD4 mRNA and protein expression was decreased in PP-Me-treated or sh-CBR1-infected quiescent cells (Figs. 4h, 4i, and S3j), demonstrating that SETD4 was involved in promoting quiescence in NSCLC cells.

3.5 SETD4-mediated maintenance of NSCLC stemness and antagonism of CBR1 inhibition

To determine whether SETD4 mediates the biological behavior of CBR1, we established SETD4-downregulated A549 and PC9 cells using a gene interference strategy (Fig. 5a). Consequently, the growth

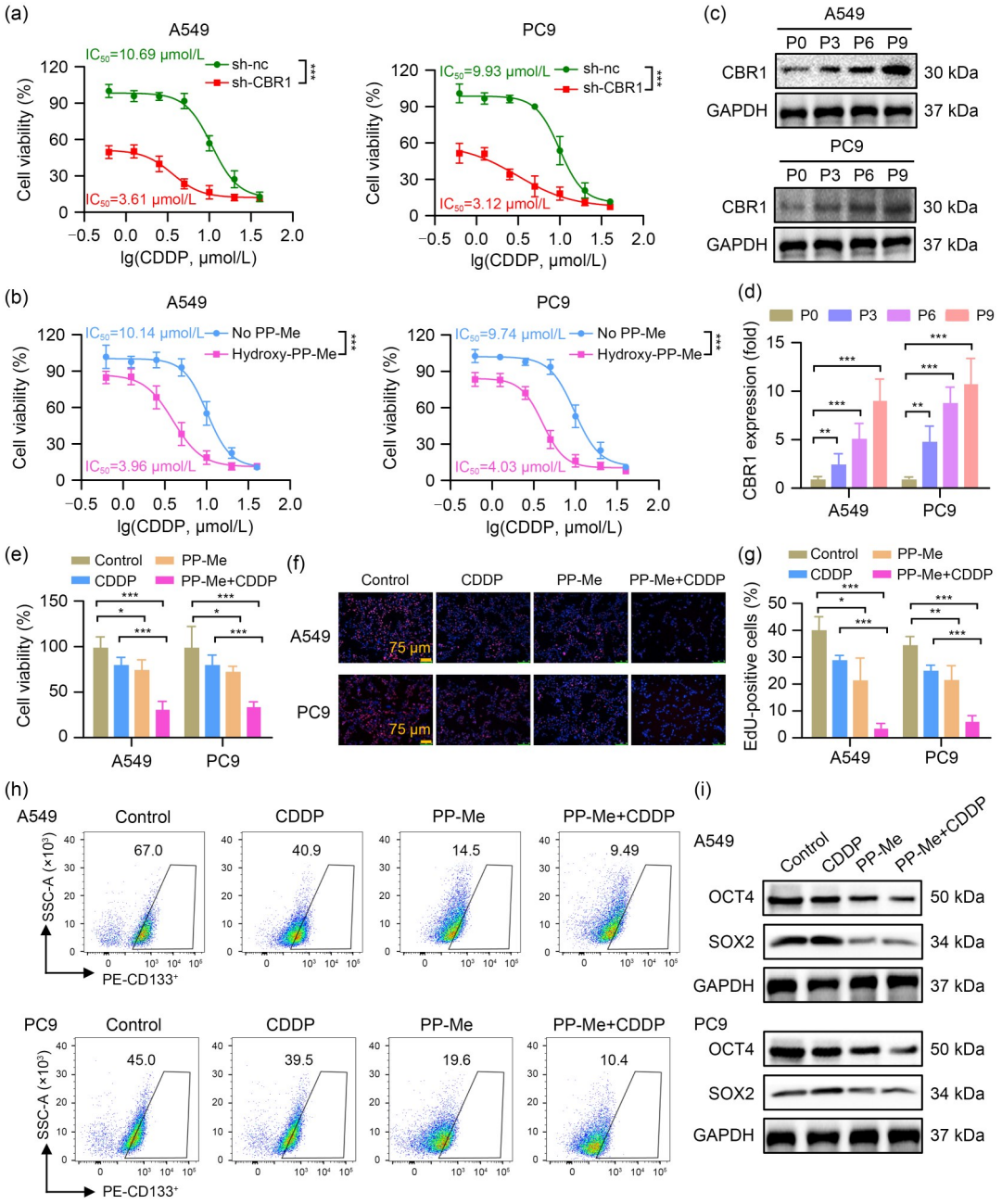

Fig. 3 Effects of CBR1 inhibition on the chemosensitivity of CDDP in NSCLC cells. (a) The IC_{50} of CDDP (μmol/L) in sh-CBR1-infected NSCLC cells. (b) The IC_{50} of CDDP in NSCLC cells treated with or without PP-Me. (c) Western blot analysis of CBR1 in NSCLC cells with or without treatment of CDDP. P0, P3, P6, and P9 represent passage 0, passage 3, passage 6, and passage 9, respectively. (d) Statistical analysis of the expression of CBR1. (e) Viability of NSCLC cells treated with CDDP, PP-Me, and the combination of PP-Me and CDDP. (f) Representative images of EdU staining of NSCLC cells treated with CDDP, PP-Me, and the combination of PP-Me and CDDP. (g) Statistical analysis of the percentage of EdU-positive cells. (h) FCM analysis of the CD133-positive cells treated with CDDP, PP-Me, and the combination of PP-Me and CDDP. (i) Western blot analysis of OCT4 and SOX2 in NSCLC cells treated with CDDP, PP-Me, and the combination of PP-Me and CDDP. The data were expressed as mean±SD, *n*=3. One-way ANOVA with Dunnett's multiple comparisons test was used. * *P*<0.05, ** *P*<0.01, *** *P*<0.001. CBR1: carbonyl reductase 1; CDDP: cisplatin; NSCLC: non-small cell lung cancer; IC_{50}: half maximal inhibitory concentration; sh-nc: short hairpin RNA (shRNA) negative control; sh-CBR1: shRNA CRB1; GAPDH: glyceraldehyde-3-phosphate dehydrogenase; PP-Me: hydroxy-PP-Me; EdU: 5-ethynyl-2'-deoxyuridine; FCM: flow cytometer; OCT4: octamer-binding transcription factor 4; SOX2: SRY (sex determining region Y)-box 2; CD133: cluster of differentiation 133; PE-CD133: phycoerythrin-conjugated antibody of CD133; SSC-A: side scatter-area; ANOVA: analysis of variance; SD: standard deviation.

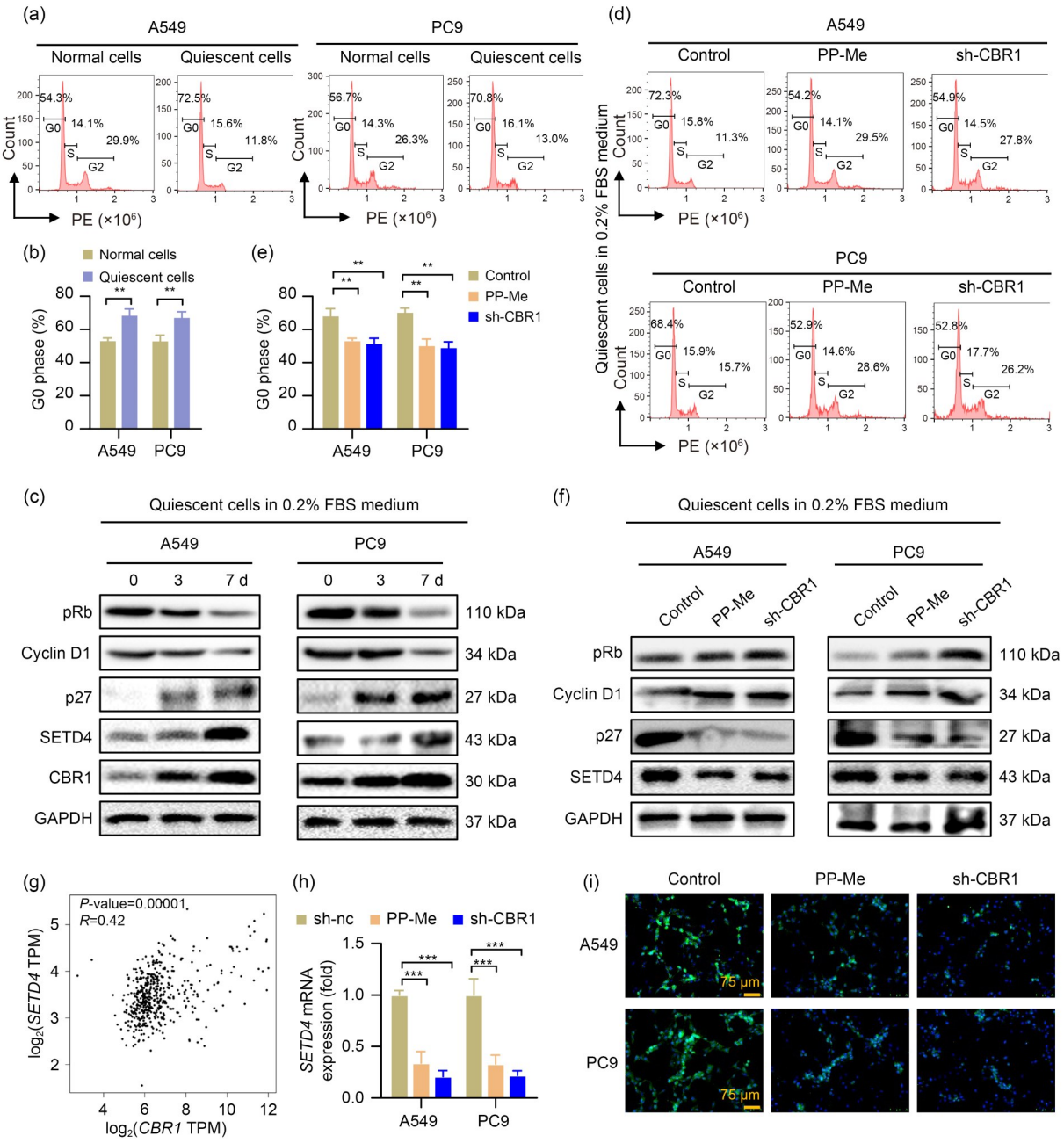

Fig. 4 Effects of CBR1 on quiescence of NSCLC cells. (a) FCM analysis of the cycles in non-quiescent and quiescent cells. (b) The percentage of G0 phase cells in non-quiescent and quiescent cells. (c) Western blot analysis of pRb, cyclin D1, p27, SETD4, and CBR1 in non-quiescent and quiescent cells. (d) FCM analysis of the cycles in sh-CBR1-infected and PP-Me-treated quiescent cells. (e) The percentage of cells in the G0 phase. (f) Western blot analysis of pRb, cyclin D1, p27, and SETD4 in sh-CBR1-infected and PP-Me-treated quiescent cells. (g) The association between the mRNA expression of *SETD4* and *CBR1* in NSCLC samples from the TCGA database. (h) qPCR analysis of *SETD4* mRNA in sh-CBR1-infected and PP-Me-treated quiescent cells. (i) Cells treated with PP-Me or infected with sh-CBR1 were stained with SETD4 antibody for immunofluorescence analysis. The data were expressed as mean±SD, n=3. One-way ANOVA with Dunnett's multiple comparisons test was used. ** P<0.01, *** P<0.001. CBR1: carbonyl reductase 1; NSCLC: non-small cell lung cancer; FCM: flow cytometer; TCGA: The Cancer Genome Atlas; qPCR: quantitative polymerase chain reaction; sh-nc: short hairpin RNA (shRNA) negative control; sh-CBR1: shRNA CRB1; PP-Me: hydroxy-PP-Me; pRb: phospho-retinoblastoma; p27: cyclin-dependent kinase inhibitor 1B; SETD4: SET domain-containing protein 4; FBS: fetal bovine serum; GAPDH: glyceraldehyde-3-phosphate dehydrogenase; mRNA: messenger RNA; TPM: transcripts per million; ANOVA: analysis of variance; SD: standard deviation.

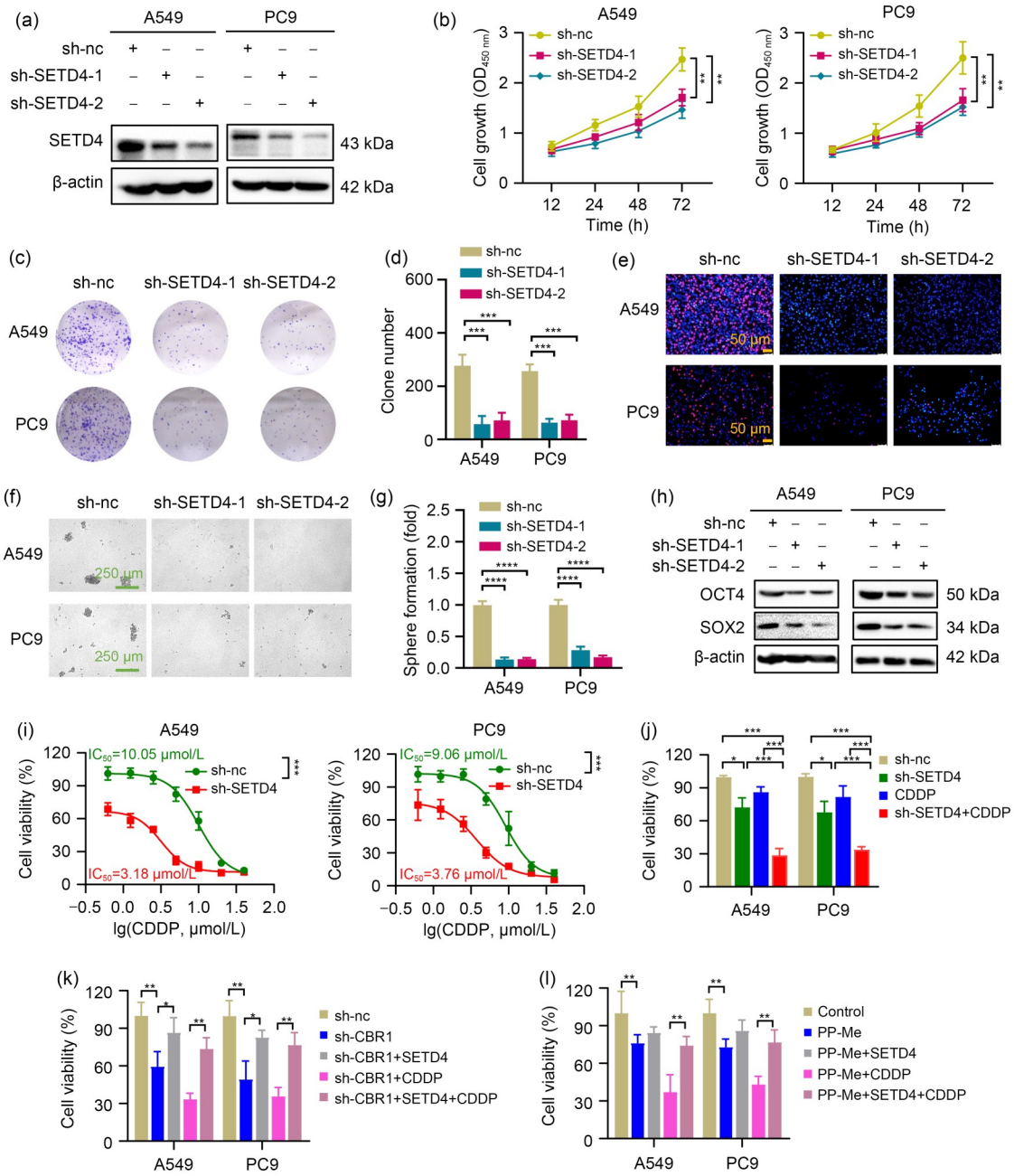

Fig. 5 Oncogenic effects of CBR1 mediated by SETD4. (a) Gene interference strategy applied to knock down the expression of SETD4. (b) Cell viability was tested using CCK-8 assay. (c) Visualization of clones. (d) Statistical analysis of the clone number. (e) Visualization of EdU-positive cells. (f) Representative images of sphere formation in sh-SETD4-1- and sh-SETD4-2-infected CSCs. (g) Relative sphere formation ability of sh-SETD4-1- and sh-SETD4-2-infected CSCs. (h) Western blot analysis of OCT4 and SOX2. (i) The IC_{50} of CDDP (μmol/L) in sh-SETD4-infected NSCLC cells. (j) The viability of cells with sh-SETD4 infection, CDDP treatment, or sh-SETD4 infection plus CDDP treatment. (k) The viability of sh-CBR1-infected cells and sh-CBR1 plus SETD4-overexpressed plasma-infected cells with or without CDDP treatment. (l) The viability of PP-Me-treated cells and PP-Me treated plus SETD4-overexpressed plasma-infected cells with or without CDDP treatment. The data were expressed as mean±SD, *n*=3. One-way ANOVA with Dunnett's multiple comparisons test was used. * *P*<0.05, ** *P*<0.01, * *P*<0.001, **** *P*<0.0001. SETD4: SET domain-containing protein 4; CBR1: carbonyl reductase 1; sh-nc: short hairpin RNA (shRNA) negative control; sh-CBR1: short hairpin RNA (shRNA) CRB1; sh-SETD4: shRNA SETD4; CCK-8: cell counting kit-8; EdU: 5-ethynyl-2'-deoxyuridine; CSCs: cancer stem cells; OCT4: octamer-binding transcription factor 4; SOX2: SRY (sex determining region Y)-box 2; GAPDH: glyceraldehyde-3-phosphate dehydrogenase; $OD_{450\ nm}$: optical density at 450 nm; IC_{50}: half maximal inhibitory concentration; CDDP: cisplatin; PP-Me: hydroxy-PP-Me; ANOVA: analysis of variance; SD: standard deviation.**

rate (Fig. 5b), clony formation ability (Figs. 5c and 5d), and percentage of EdU-positive cells (Figs. 5e and S4a) in SETD4-infected cells were decreased, compared to negative control cells. Additionally, SETD4 downregulation led to a decreased capacity of sphere formation (Figs. 5f and 5g) and expression of OCT4 and SOX2 (Figs. 5h, S4b, and S4c). Furthermore, SETD4 downregulation led to a decrease in the IC_{50} of CDDP from 10.05 to 3.18 μmol/L in A549 cells and from 9.06 to 3.76 μmol/L in PC9 cells (Fig. 5i). The CCK-8 results confirmed that the viability of sh-SETD4-infected cells treated with CDDP was lower than that observed in negative control cells subjected to CDDP treatment (Fig. 5j). These results showed that SETD4 inhibition can hinder the stemness of NSCLC cells and increase their chemosensitivity to CDDP. To confirm that SETD4 mediated the chemosensitivity of CBR1 inhibition, SETD4-overexpressing plasma was transfected to sh-nc- or sh-CBR1-infected A549 and PC9 cells (Fig. S4d). The CCK-8 results indicated that SETD4 overexpression alleviated the growth inhibition and increased the chemosensitivity effects of CBR1 inhibition by sh-CBR1 and PP-Me (Figs. 5k and 5l).

3.6 Antitumor efficacy of PP-Me and CDDP in vivo

A549 cells were subcutaneously injected into the mice. The mice were categorized into four groups: control group, CDDP group, PP-Me group, and PP-Me plus CDDP group. The tumor volume and body weight of the mice were monitored every three days. The mice were sacrificed on Day 21, and the tumor tissues were collected (Fig. 6a). The tumor weight and volume showed a slight decrease in the CDDP and PP-Me groups. The combined treatment with PP-Me and CDDP resulted in a much stronger reduction in tumor size and weight than the individual treatments with either PP-Me or CDDP alone (Figs. 6b and 6c). Significantly, the body weights of all mice did not show a significant decline, demonstrating that the combined therapy did not cause severe toxicity (Fig. 6d). Western blot analysis revealed that the expression of OCT4 and SOX2 was effectively inhibited in both the PP-Me group and the PP-Me plus CDDP group, demonstrating the anti-stemness capacity of PP-Me (Figs. 6e and 6g). Indeed, the expression of SETD4 was decreased in the PP-Me group and the PP-Me plus CDDP group, highlighting the anti-quiescence capacity of PP-Me (Figs. 6e and 6g). For verification, the expression of OCT4, SOX2, and SETD4 was analyzed using immunohistochemistry. Consistent with the western blot results, their expression was decreased in the PP-Me group and the PP-Me plus CDDP group, indicating the anti-stemness and anti-quiescence effects of CBR1 inhibition in vivo (Figs. 6f and 6h).

4 Discussion

The expression of CBR1 in various cancer types has been studied, and research findings indicate that it can vary across different cancers, including breast (Morin-Buote et al., 2021), lung (Kalabus et al., 2012), gastrointestinal (Matsunaga et al., 2015), endometrial (Murakami et al., 2012), ovarian (Osawa et al., 2015), liver (Tak et al., 2011), and pancreatic (Zhou et al., 2021) cancers, and leukemia (Jang et al., 2012). Specifically, the overexpression of CBR1 in lung cancer tissues has been associated with poor prognosis and aggressive tumor behavior (Kalabus et al., 2012; Koczurkiewicz-Adamczyk et al., 2020). In this study, based on data from the TCGA database and our western blot results of clinical samples, we verified that the expression of CBR1 is upregulated in NSCLC tissue and high expression of CBR1 indicates a poor prognosis for NSCLC patients, consistent with a previous study (Kalabus et al., 2012). Additionally, the upregulated expression of CBR1 in NSCLC cell lines was confirmed using western blot. To further investigate the biofunctions of CBR1, we focused on the CSCs, which have been implicated as a cause of tumor progression and treatment resistance. The novelty of this study indicated that the expression of CBR1 was upregulated and the knockdown of CBR1 led to a reduction in the number of CD133-positive cells and the expression of stem cell-related proteins, including OCT4 and SOX2, indicating the stemness maintenance property of CBR1.

Although various agents, including immunomodulators and molecular targeted drugs, prolong the OS of NSCLC patients, platinum-based chemotherapy strategies still play an important role in clinical practice (Iwamoto et al., 2015; Niho et al., 2020). CDDP is commonly used in the treatment of NSCLC and works by interfering with DNA in cancer cells, preventing the cells from dividing and growing. CDDP resistance remains a significant challenge. Many factors, such as

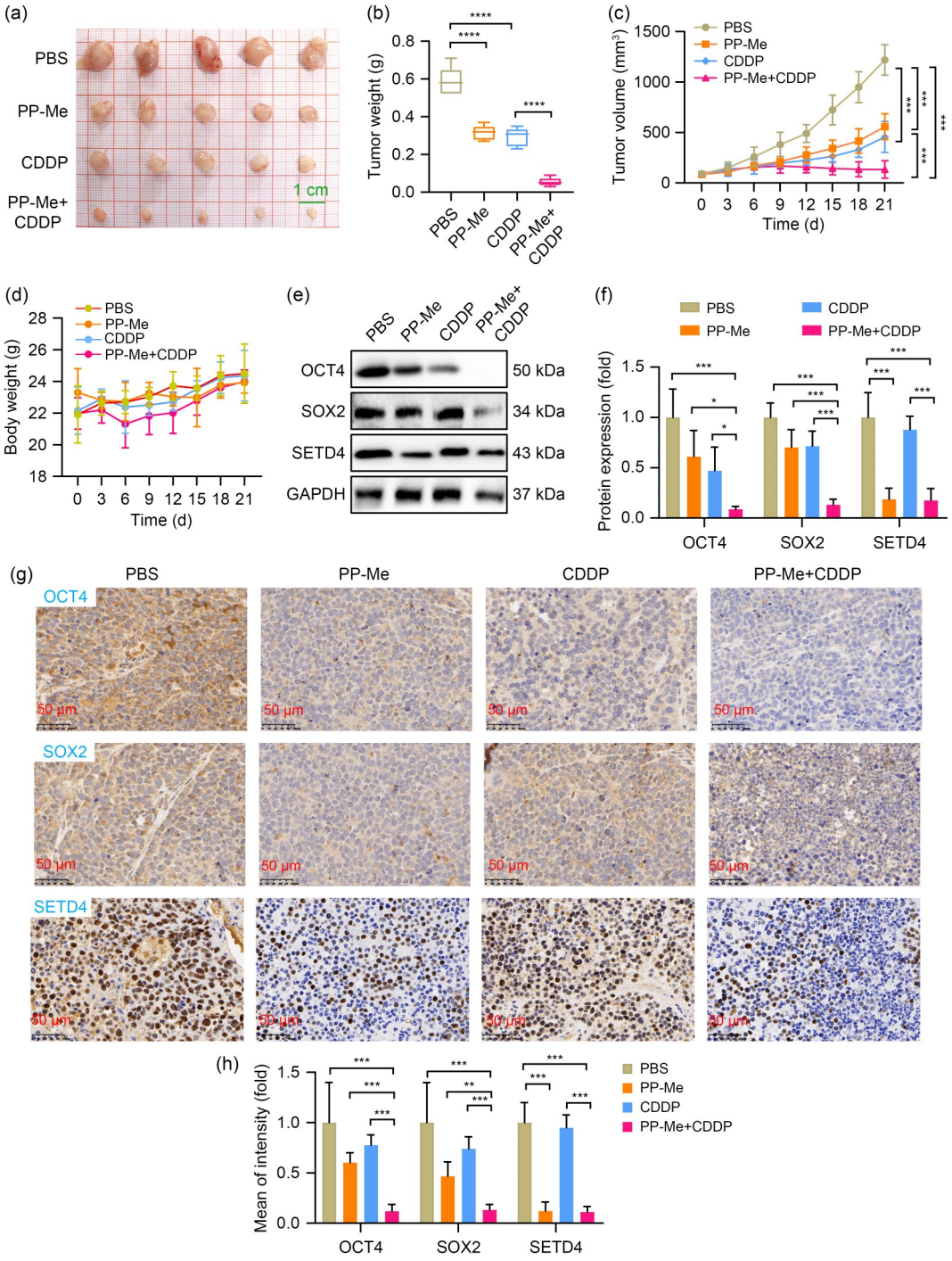

Fig. 6 Antitumor effect of CDDP increased by PP-Me in xenograft bearing mice. (a) Mice were sacrificed at 21 d and the tumor masses were collected. (b, c) The tumor weights (b) and volumes (c) were compared. (d) The body weights of the different groups showed no significant difference. (e, f) Western blot analysis and quantitative results of the expression of OCT4, SOX2, and SETD4 in tumor tissues with PP-Me, CDDP, or PP-Me plus CDDP treatment. (g, h) Immunohistochemistry analysis and quantitative results of the expression of OCT4, SOX2, and SETD4 in tumor tissues with PP-Me, CDDP, or PP-Me plus CDDP treatment. The data were expressed as mean±SD, *n*=3. One-way ANOVA with Dunnett's multiple comparisons test was used. * *P*<0.05, ** *P*<0.01, *** *P*<0.001, **** *P*<0.0001. PP-Me: hydroxy-PP-Me; CDDP: cisplatin; OCT4: octamer-binding transcription factor 4; SOX2: SRY (sex determining region Y)-box 2; SETD4: SET domain-containing protein 4; GAPDH: glyceraldehyde-3-phosphate dehydrogenase; PBS: phosphate-buffered saline; ANOVA: analysis of variance; SD: standard deviation.

reduced drug accumulation, increased DNA repair, epigenetic alterations, microenvironmental changes, and CSCs, may contribute to resistance (Galluzzi et al., 2012). Based on the stemness maintenance property of CBR1, we investigated the role of CBR1 in chemosensitivity to CDDP. The TCGA data also suggested that high expression of CBR1 is associated with a shorter PPS in patients receiving chemotherapy. As a reductase, CBR1 may facilitate the reduction of doxorubicin, a common chemotherapy agent, to doxorubicinol, which could enhance DOX-induced toxicity in cardiomyocytes but decrease its antineoplastic effects in breast cancer (Jo et al., 2017). Indeed, similar functions of CBR1 in NSCLC were reported by Koczurkiewicz-Adamczyk et al. (2020, 2022). Fortunately, the inhibition of CBR1 by cinnamamide derivatives could contribute to cardiomyocyte protection and chemosensitivity (Koczurkiewicz-Adamczyk et al., 2020, 2022). As expected, we confirmed that CBR1 was associated with the cytotoxicity of CDDP. Increased expression of CBR1 was observed in CDDP-treated NSCLC cells, demonstrating its potential role in chemotherapy resistance. The combination of PP-Me and CDDP resulted in a sharp decrease of the stemness property both in vitro and in vivo. These results highlight that increased chemosensitivity may be related to reduced stemness following CBR1 inhibition.

Considering that quiescence in CSCs is thought to be a protective mechanism that allows these cells to evade the cytotoxic effects of chemotherapy (Ye et al., 2019; Mukhopadhyay et al., 2023; Wang et al., 2023), we further investigated the role of CBR1 in promoting quiescence. We found that CBR1 was upregulated in quiescent cells. CBR1 inhibition may reverse this progression, as shown by the increase in cyclin D1 and pRb, and the decrease in p27 and SETD4 in NSCLC cells treated with PP-ME or sh-CBR1. Notably, altered DNA methylation is commonly found in quiescent cells to maintain the integrity of cellular function. SETD4 is a member of the histone-lysine *N*-methyltransferase family, known for its role in catalyzing the trimethylation of Lys-20 of histone H4 and thereby facilitating heterochromatin formation (Dai et al., 2017; Zhong et al., 2019). SETD4 serves as a regulator involved in various biofunctions of cancer cells (Zhu et al., 2016; Zhang et al., 2022) and is associated with the stem cell property (Dai et al., 2017; Liao et al., 2021; Cai et al., 2022). Indeed, SETD4 serves as a biomarker of quiescence in CSCs. Thus, we wanted to determine the role of SETD4 in CBR1-mediated chemosensitivity.

Our results confirmed that SETD4 is upregulated in quiescent cells. Notably, we observed a positive correlation between the expression of CBR1 and that of SETD4. CBR1 inhibition led to a reduction in SETD4 levels in vitro and in vivo. Sustained expression of SETD4 in NSCLC cells appeared to mitigate the increased chemosensitivity induced by CBR1 inhibition, highlighting the critical role of SETD4 as a downstream effector of CBR1. Collectively, our findings indicate that the CBR1-SETD4 axis plays a vital role in maintaining CSC properties and promoting chemotherapy resistance. Inhibition of SETD4 not only reduces stemness but also sensitizes NSCLC cells to chemotherapy, suggesting that CBR1-induced SETD4 expression facilitates quiescence and shields CSCs from cytotoxic stress.

Our insights into the molecular interplay between CBR1 and SETD4 advance the understanding of NSCLC progression and therapeutic resistance. The CBR1-SETD4 axis may emerge as a promising target for overcoming chemotherapy resistance, particularly in quiescent CSCs. However, our study has several limitations. For example, the interactions of CBR1 with other genes and signaling pathways, such as phosphatidylinositol 3-kinase/protein kinase B (PI3K/Akt), mitogen-activated protein kinase/extracellular signal-regulated kinase (MAPK/ERK), nuclear factor-κB (NF-κB), Wnt/β-catenin, and Janus kinase/signal transducer and activator of transcription (JAK/STAT) pathways, known to be involved in stemness and quiescence, should be investigated to better understand the broader regulatory network (Shi and Di, 2017). These genes and signaling pathways could help identify new ways to treat NSCLC, particularly through combination therapies involving cannabinoids, immune modulation, and targeted therapies. Furthermore, research on the specific molecular mechanisms underlying these interactions will be crucial in determining whether CBR1 could serve as a promising therapeutic target in NSCLC. More sophisticated preclinical models, such as genetically engineered mouse models, should be applied to validate the findings. Furthermore, identifying potential biomarkers that could predict the response to CBR1 inhibition will help stratify patients who are likely to benefit from such therapies. Thus, more efforts should be made, including investigating specific

molecular mechanisms underlying the interactions between quiescent cells, CSCs, and chemotherapy resistance in NSCLC. The long-term effects of this novel therapy on patient survival, quality of life, and potential side effects should be investigated using animal models that more closely mimic human NSCLC. In addition, further studies validating the identified biomarkers in larger and more diverse patient cohorts and exploring the clinical applicability of personalized treatment strategies should be conducted. Preclinical studies should be performed to assess the efficacy of targeted therapies aimed at reducing cancer stemness and quiescence by inhibiting CBR1.

In conclusion, our study revealed that CBR1 is significantly overexpressed in NSCLC and plays a crucial role in maintaining the self-renewal capacity of CSCs. CBR1 inhibition not only impairs growth but also increases chemotherapeutic sensitivity to CDDP in NSCLC. Furthermore, CBR1 inhibition opposes the quiescence of NSCLC cells and involves the alteration of SETD4. SETD4 may be a downstream target of CBR1, mediating stemness and chemotherapy resistance in NSCLC.

Data availability statement

All datasets analyzed in this study are available from the corresponding author upon request.

Acknowledgments

This study was supported by the National Natural Science Foundation of China (No. 82170054) and the Natural Science Foundation of Zhejiang Province (No. Y21H010014), China. We thank all patients involved in this study. We also thank all friends and colleagues who offered their kind help but are not listed as authors of this study.

Author contributions

All authors contributed to the study conception and design. Material preparation, data collection, and analysis were performed by Weiwen LI, Jialu ZHAO, Weihong LAN, and Xiaofei YE. The first draft of the manuscript was written by Weiwen LI and Jialu ZHAO, and revised by Kejing YING. All authors have read and approved the final manuscript, and therefore, have full access to all the data in the study and take responsibility for the integrity and security of the data.

Compliance with ethics guidelines

Weiwen LI, Jialu ZHAO, Weihong LAN, Xiaofei YE, and Kejing YING declare that they have no conflicts of interest.

This study was performed in line with the principles of the 1964 Declaration of Helsinki and its later amendments or comparable ethical standards. Approval was granted by the Ethics Committee of the Fifth Affiliated Hospital of Wenzhou Medical University (No. 2020D133).

References

Bray JE, Marsden BD, Oppermann U, 2009. The human short-chain dehydrogenase/reductase (SDR) superfamily: a bioinformatics summary. *Chem Biol Interact*, 178(1-3): 99-109. https://doi.org/10.1016/j.cbi.2008.10.058

Brody H, 2020. Lung cancer. *Nature*, 587(7834):S7. https://doi.org/10.1038/d41586-020-03152-0

Cai SL, Yang YS, Ding YF, et al., 2022. SETD4 cells contribute to brain development and maintain adult stem cell reservoir for neurogenesis. *Stem Cell Reports*, 17(9):2081-2096. https://doi.org/10.1016/j.stemcr.2022.07.017

Chen G, Zhang HH, Sun HX, et al., 2023a. Bufalin targeting BFAR inhibits the occurrence and metastasis of gastric cancer through PI3K/AKT/mTOR signal pathway. *Apoptosis*, 28(9-10):1390-1405. https://doi.org/10.1007/s10495-023-01855-z

Chen G, Yang LN, Liu GX, et al., 2023b. Research progress in protein microarrays: focussing on cancer research. *Proteom Clin Appl*, 17(1):2200036. https://doi.org/10.1002/prca.202200036

Chen KC, Zhang CZ, Ling SB, et al., 2021. The metabolic flexibility of quiescent CSC: implications for chemotherapy resistance. *Cell Death Discov*, 12(9):835. https://doi.org/10.1038/s41419-021-04116-6

Dai L, Ye S, Li HW, et al., 2017. SETD4 regulates cell quiescence and catalyzes the trimethylation of H4K20 during diapause formation in *Artemia*. *Mol Cell Biol*, 37(7): e00453-16. https://doi.org/10.1128/MCB.00453-16

Galluzzi L, Senovilla L, Vitale I, et al., 2012. Molecular mechanisms of cisplatin resistance. *Oncogene*, 31(15):1869-1883. https://doi.org/10.1038/onc.2011.384

Heng WS, Gosens R, Kruyt FAE, 2019. Lung cancer stem cells: origin, features, maintenance mechanisms and therapeutic targeting. *Biochem Pharmacol*, 160:121-133. https://doi.org/10.1016/j.bcp.2018.12.010

Herz HM, Garruss A, Shilatifard A, 2013. SET for life: biochemical activities and biological functions of SET domain-containing proteins. *Trends Biochem Sci*, 38(12):621-639. https://doi.org/10.1016/j.tibs.2013.09.004

Iwamoto Y, Mitsudomi T, Sakai K, et al., 2015. Randomized phase II study of adjuvant chemotherapy with long-term S-1 versus cisplatin+S-1 in completely resected stage II-IIIA non-small cell lung cancer. *Clin Cancer Res*, 21(23): 5245-5252. https://doi.org/10.1158/1078-0432.CCR-14-3160

Jang M, Kim Y, Won H, et al., 2012. Carbonyl reductase 1 offers a novel therapeutic target to enhance leukemia treatment by arsenic trioxide. *Cancer Res*, 72(16):4214-4224. https://doi.org/10.1158/0008-5472.CAN-12-1110

Jiang X, Li Y, Feng JL, et al., 2020. Safrana l prevents prostate cancer recurrence by blocking the re-activation of

quiescent cancer cells *via* downregulation of S-phase kinase-associated protein 2. *Front Cell Dev Biol*, 8:598620. https://doi.org/10.3389/fcell.2020.598620

Jo A, Choi TG, Jo YH, et al., 2017. Inhibition of carbonyl reductase 1 safely improves the efficacy of doxorubicin in breast cancer treatment. *Antioxid Redox Sign*, 26(2):70-83. https://doi.org/10.1089/ars.2015.6457

Kalabus JL, Cheng QY, Jamil RG, et al., 2012. Induction of carbonyl reductase 1 (*CBR1*) expression in human lung tissues and lung cancer cells by the cigarette smoke constituent benzo[*a*]pyrene. *Toxicol Lett*, 211(3):266-273. https://doi.org/10.1016/j.toxlet.2012.04.006

Kavanagh KL, Jörnvall H, Persson B, et al., 2008. Medium- and short-chain dehydrogenase/reductase gene and protein families: the SDR superfamily: functional and structural diversity within a family of metabolic and regulatory enzymes. *Cell Mol Life Sci*, 65(24):3895. https://doi.org/10.1007/s00018-008-8588-y

Koczurkiewicz-Adamczyk P, Piska K, Gunia-Krzyżak A, et al., 2020. Cinnamic acid derivatives as chemosensitising agents against DOX-treated lung cancer cells – involvement of carbonyl reductase 1. *Eur J Pharm Sci*, 154:105511. https://doi.org/10.1016/j.ejps.2020.105511

Koczurkiewicz-Adamczyk P, Gąsiorkiewicz B, Piska K, et al., 2022. Cinnamamide derivatives with 4-hydroxypiperidine moiety enhance effect of doxorubicin to cancer cells and protect cardiomyocytes against drug-induced toxicity through CBR1 inhibition mechanism. *Life Sci*, 305:120777. https://doi.org/10.1016/j.lfs.2022.120777

Lal S, Sandanaraj E, Wong ZW, et al., 2008. *CBR1* and *CBR3* pharmacogenetics and their influence on doxorubicin disposition in Asian breast cancer patients. *Cancer Sci*, 99(10):2045-2054. https://doi.org/10.1111/j.1349-7006.2008.00903.x

Liao XM, Wu CX, Shao ZM, et al., 2021. SETD4 in the proliferation, migration, angiogenesis, myogenic differentiation and genomic methylation of bone marrow mesenchymal stem cells. *Stem Cell Rev Rep*, 17(4):1374-1389. https://doi.org/10.1007/s12015-021-10121-1

Massey AJ, Benwell K, Burbridge M, et al., 2021. Targeting DYRK1A/B kinases to modulate p21-cyclin D1-p27 signalling and induce anti-tumour activity in a model of human glioblastoma. *J Cell Mol Med*, 25(22):10650-10662. https://doi.org/10.1111/jcmm.17002

Matsunaga T, Kezuka C, Morikawa Y, et al., 2015. Up-regulation of carbonyl reductase 1 renders development of doxorubicin resistance in human gastrointestinal cancers. *Biol Pharm Bull*, 38(9):1309-1319. https://doi.org/10.1248/bpb.b15-00176

Miller M, Hanna N, 2021. Advances in systemic therapy for non-small cell lung cancer. *BMJ*, 375:n2363. https://doi.org/10.1136/bmj.n2363

Morin-Buote J, Ennour-Idrissi K, Poirier É, et al., 2021. Association of breast tumour expression of cannabinoid receptors CBR1 and CBR2 with prognostic factors and survival in breast cancer patients. *J Pers Med*, 11(9):852. https://doi.org/10.3390/jpm11090852

Mukhopadhyay D, Goel HL, Xiong CA, et al., 2023. The calcium channel TRPC6 promotes chemotherapy-induced persistence by regulating integrin α6 mRNA splicing. *Cell Rep*, 42(11):113347. https://doi.org/10.1016/j.celrep.2023.113347

Murakami A, Yakabe K, Yoshidomi K, et al., 2012. Decreased carbonyl reductase 1 expression promotes malignant behaviours by induction of epithelial mesenchymal transition and its clinical significance. *Cancer Lett*, 323(1):69-76. https://doi.org/10.1016/j.canlet.2012.03.035

Niho S, Yoshida T, Akimoto T, et al., 2020. Randomized phase II study of chemoradiotherapy with cisplatin + S-1 versus cisplatin + pemetrexed for locally advanced non-squamous non-small cell lung cancer: SPECTRA study. *Lung Cancer*, 141:64-71. https://doi.org/10.1016/j.lungcan.2020.01.008

Oppermann U, 2007. Carbonyl reductases: the complex relationships of mammalian carbonyl- and quinone-reducing enzymes and their role in physiology. *Annu Rev Pharmacol Toxicol*, 47(1):293-322. https://doi.org/10.1146/annurev.pharmtox.47.120505.105316

Osawa Y, Yokoyama Y, Shigeto T, et al., 2015. Decreased expression of carbonyl reductase 1 promotes ovarian cancer growth and proliferation. *Int J Oncol*, 46(3):1252-1258. https://doi.org/10.3892/ijo.2014.2810

Pennycook BR, Barr AR, 2020. Restriction point regulation at the crossroads between quiescence and cell proliferation. *FEBS Lett*, 594(13):2046-2060. https://doi.org/10.1002/1873-3468.13867

Piska K, Koczurkiewicz P, Wnuk D, et al., 2019. Synergistic anticancer activity of doxorubicin and piperlongumine on DU-145 prostate cancer cells – the involvement of carbonyl reductase 1 inhibition. *Chem Biol Interact*, 300:40-48. https://doi.org/10.1016/j.cbi.2019.01.003

Schlager JJ, Powis G, 1990. Cytosolic NAD(P)H:(Quinone-acceptor)oxidoreductase in human normal and tumor tissue: effects of cigarette smoking and alcohol. *Int J Cancer*, 45(3):403-409. https://doi.org/10.1002/ijc.2910450304

Shi SM, Di L, 2017. The role of carbonyl reductase 1 in drug discovery and development. *Expert Opin Drug Metab Toxicol*, 13(8):859-870. https://doi.org/10.1080/17425255.2017.1356820

Siegel RL, Miller KD, Fuchs HE, et al., 2021. Cancer statistics, 2021. *CA A Cancer J Clin*, 71(1):7-33. https://doi.org/10.3322/caac.21654

Tak E, Lee S, Lee J, et al., 2011. Human carbonyl reductase 1 upregulated by hypoxia renders resistance to apoptosis in hepatocellular carcinoma cells. *J Hepatol*, 54(2):328-339. https://doi.org/10.1016/j.jhep.2010.06.045

Wang YH, Yu YM, Yang WJ, et al., 2023. SETD4 confers cancer stem cell chemoresistance in nonsmall cell lung cancer patients via the epigenetic regulation of cellular quiescence. *Stem Cells Int*, 2023:7367854. https://doi.org/10.1155/2023/7367854

Ye S, Ding YF, Jia WH, et al., 2019. SET domain-containing protein 4 epigenetically controls breast cancer stem cell quiescence. *Cancer Res*, 79(18):4729-4743. https://doi.org/10.1158/0008-5472.CAN-19-1084

Zhang HH, Zhang Z, Guo TT, et al., 2023a. Annexin A protein family: focusing on the occurrence, progression and treatment of cancer. *Front Cell Dev Biol*, 11:1141331. https://doi.org/10.3389/fcell.2023.1141331

Zhang HH, Dong XL, Ding XY, et al., 2023b. Bufalin targeting CAMKK2 inhibits the occurrence and development of intrahepatic cholangiocarcinoma through Wnt/β-catenin signal pathway. *J Transl Med*, 21:900. https://doi.org/10.1186/s12967-023-04613-6

Zhang YJ, Zhang HX, Zhang XL, et al., 2022. CBR3-AS1 accelerates the malignant proliferation of gestational choriocarcinoma cells by stabilizing SETD4. *Dis Markers*, 2022: 7155525. https://doi.org/10.1155/2022/7155525

Zhong YY, Ye P, Mei ZZ, et al., 2019. The novel methyltransferase SETD4 regulates TLR agonist-induced expression of cytokines through methylation of lysine 4 at histone 3 in macrophages. *Mol Immunol*, 114:179-188. https://doi.org/10.1016/j.molimm.2019.07.011

Zhou L, Yang C, Zhong WL, et al., 2021. Chrysin induces autophagy-dependent ferroptosis to increase chemosensitivity to gemcitabine by targeting CBR1 in pancreatic cancer cells. *Biochem Pharmacol*, 193:114813. https://doi.org/10.1016/j.bcp.2021.114813

Zhu SX, Xu YP, Song M, et al., 2016. PRDM16 is associated with evasion of apoptosis by prostatic cancer cells according to RNA interference screening. *Mol Med Rep*, 14(4): 3357-3361. https://doi.org/10.3892/mmr.2016.5605

Supplementary information

Figs. S1–S4